Biomechanical study of a drop foot brace

Mikkelsen, Lars Pilgaard; Skorini, Ragnhild Í; Løgstrup Andersen, Tom

Published in:
Proceedings

Publication date:
2011

Document Version
Publisher's PDF, also known as Version of record

Biomechanical study of a drop foot brace

Lars P. Mikkelsen, Ragnhild Í Skorini and Tom L. Andersen

Materials Research Div., Risø DTU, Technical University of Denmark

Abstract: A person specific drop foot brace was simulated in the commercial finite element code Abaqus.The geometry was imported from a 3D optical scan of the actual surface and modeled as a composite material layup defined in a local discrete material coordinate system. The finite element model was used in order to model the stance phase in a normal walking. The material choice is a challenging task giving flexibility to the brace together with sufficiently stiffness and fatigue strength. The simulation has been compared with measurements from a strain gauge mounted foot brace tested in use. Based on simulations, a large number of expensive trial and error iterations can be avoided. Simulations show a strong geometry interaction with the loading of the material.

Keywords: Medico, composite materials, shell model, STL file import.

1. Introduction

Drop foot is a reduced or lack of action from the muscles that lift the foot (Kottnik, 2007). When these muscles lack function they are unable to dorsiflex the ankle which causes the foot to be dragged on the ground. For some people the lack of function is so severe that they are not able to walk without treatment, while others have a steppage gait. The recommended treatment depends on the etiology of drop foot. Sometimes surgery is necessary while some patients can be treated by wearing an ankle foot orthosis, a brace that stabilizes the foot and lifts it in an upright position while the foot swings.

A very large number of people suffering from drop foot but no exact numbers is to the authors knowledge available. Nevertheless, it can be estimated that 20 % of those surviving stroke suffer from drop foot (Wade, 1987). Worldwide 15 million people suffer from stroke every year, out of these 5 million die (Murray, 2002). This gives 2 million people suffering from drop foot only due to stroke. Many other diseases can lead to drop foot and as such the total number of people suffering from drop foot must be much higher. Approximately 30 % of all cases of drop foot are due to peroneal neuropathy (Rubin, 1998). Neural damages can be caused by trauma or nerve related injuries. The nerve roots and spinal cord are fragile to herniation of discs and other lesions of the nerves (Bojsen-Møller, 2005). Furthermore muscle impairments can lead to drop foot.

A great variety of ankle foot orthosis (also called AFO) are available on the market today. These have different designs and material properties. As shown in Fig. 1a, the ankle foot orthosis tested in this study is a person specific plastic brace with two rods, one on the lateral and one on the medial side of the ankle, see (Flexbrace, 2010). The rods are in the investigated brace reinforced with a folded and twisted carbon glass fiber webbing. The geometry of the person-specific brace is extracted by the company Zebicon (Zebicon, 2002) which performing an optic 3D scan of the inner surface of the brace, see figure 1b. The resulting STL-representation of the surface is

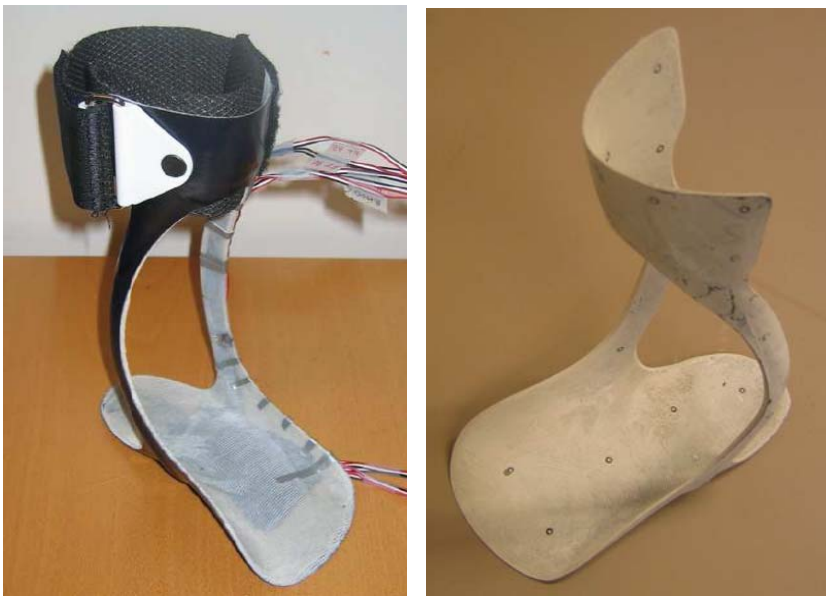

Figure 1. a) Angle foot orthosis mounted with strain gauges, b) The brace used for the 3D optical scan with reflective markers

imported as an orphan mesh defining the inner-surface of 3D shell structure into Abaqus (Simulia, 2010), see Fig 2a.

The material in the shell is modeled as a composite layup where extra carbon fiber reinforcement is placed in the rods. In Fig. 2b the fiber-reinforced part can be seen as the non-dark blue part of the brace. In the actual brace, additional fiber reinforcement was also present in the sole. This is not included in the model as the entire sole is kinematic coupled to a reference point and therefore representing a rigid part of the brace. The part coupled to the reference point in the sole is shown as the lower dark blue region in Fig. 2c. The fixture around the shin, the upper dark blue part in Fig 2c, is kinematic couple to another reference point.

Based on a loading representing a normal gait, the specific ankle foot orthosis is modeled in Abaqus. Thereby, it is possible to investigate the material selection used and compare this with other obtional materials. The material choice is a challenging task giving flexibility to the brace together with sufficiently stiffness and fatigue strength. The simulation has been compared with measurements from a strain gauge mounted foot brace tested in use. Based on simulations, a large number of expensive trial and error iterations can be avoided. Simulations show a strong geometry interaction with the loading of the material, and the loading of the two rods in the brace is not so simple as first expected.

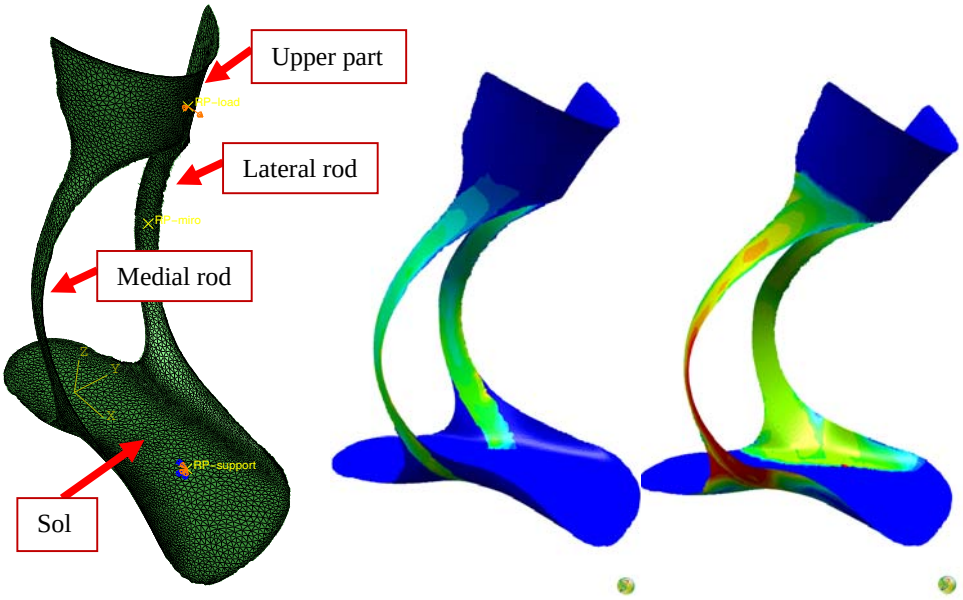

Figure 2. a) Orphan mesh model from Abaqus, b) The fiber-reinforced part of the brace shown for $U = 58mm$ c) The stress stage in the deformed brace for $U = 76mm$.

2. Materials

The brace is build up of a number of material layers which are impregnated by an acryl resin using vacuum infusion. The material layup from the inner surface is

- Three layer of perlon knitted stockinette
- In some part of the brace, additional carbon glass fiber webbing was applied
    - In the two rods; 5 mm wide webbing was folded and twisted in rolls resulting in an approximately $\pm 45^{\circ}$ fiber layup.
    - Under the heel; two 25 mm wide webbing (not included in FE-model)
    - Under the sole; three 50 mm wide webbing (not included in FE-model)
    - Across upper frontal leg; two 5 mm wide webbing (not included in FE-model)
- Additional three layer of perlon knitted stockinette in the whole brace
- One layer of knitted fabric of elasthane (a material also used in the bathing suit industry)

The carbon glass fiber webbing is a web of carbon fibers and thin glass fibers in the longitudinal direction and thin glass fibers in the transverse direction. The resin used for the vacuum infusion was customized for the carbon glass fiber webbing. In addition to the specific material layup used in the brace, three other cases has been analyzed where the twisted carbon glass webs has been

replaced. Therefore, in total results from four different material layups will be presented in the finite element simulations

1. 45-Carbon: is model with the twisted carbon glass webbing in the rods
2. UD-Carbon: is a model where the twisted carbon glass web in the rods are replaced with a folded but un-twisted carbon glass web
3. UD-Glass: the carbon glass webbing in the rods is replaced with a pure unidirectional glass fiber layup of the same thickness
4. No Fibers: There are no extra reinforcement in the rods so the brace will only be build up by 6 layer of perlon knitted stockinette ending with one layer of elasthane knitted fabric at the outer-surface of the brace.

The material properties for the acryl impregnated elasthane og perlon knitted fabric has been measured in the longitudinal and transverse direction using a standard uni-directional tensile test setup. Fig. 3 shows representative stress versus strain curves for the two materials loaded in the two directions together with the fitted curves used in the Abaqus simulation. The material behavior is approximated by a hyperelastic-plastic material law where the hyperelastic material is fitted by a third order reduced polynomial "Yeoh" material law and the subsequently plasticity is modeled with a nearly ideal plastic material law with a very flat hardening law as shown in Fig. 3 and the parameters used are given in the table in Fig. 4a.

The fiber-reinforcement of uni-directional glass fibers and the carbon glass fiber web is modeled as an orthotropic linear elastic material given by the stiffness parameters shown in Fig.4b. In order

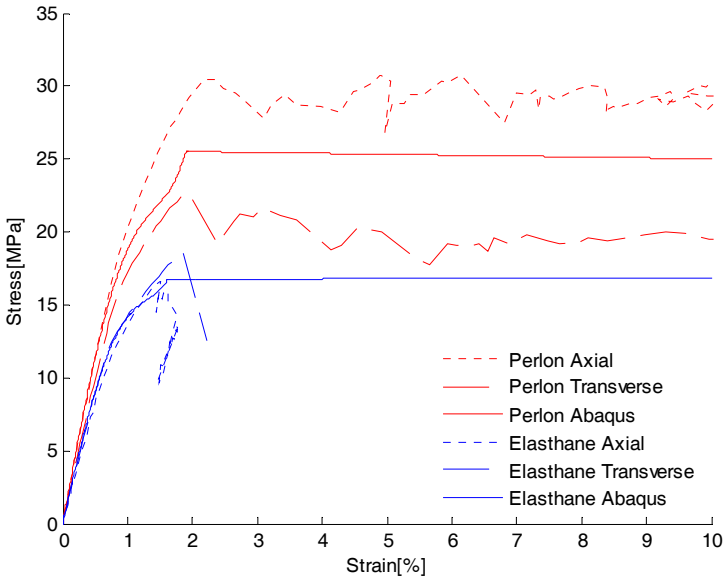

Figure 3. Representative tensile test curves and fitted models for knitted perlon and elasthane reinforced acryl.

Material	$E_{Initial}$	C_{10}	C_{20}	C_{30}	σ_y
Elasthane	1.7GPa	329MPa	-185GPa	74TPa	17MPa
Perlon	2.1GPa	407MPa	-178GPa	59TPa	26MPa

Material	E_L	E_T	ν_{LT}	G_{LT}	$G_{TT'}$
Carbon glass webbing	98.5GPa	9.8GPa	0.26	5.3GPa	1.0GPa
Unidirectional glass	27.5GPa	7.5GPa	0.32	2.3GPa	2.7GPa

Material	ε_{LU}^{+}	ε_{LU}^{-}	ε_{TU}^{+}	ε_{TU}^{-}	ε_{LTU}
Carbon glass webbing	1.2%	0.5%	0.5%	0.5%	1.0%
Unidirectional glass	2.4%	1.4%	0.7%	3.6%	4.9%

Figure 4. Material parameters used for Elasthane, Perlon, carbon and glass fiber reinforced acryl

to decide how close to failure the material is the maximum strain to failure criteria build into Abaqus has been used. In here, the parameter MSTRN is defined as

$$MSTRN = \max\left(\frac{\varepsilon_{11}}{X_\varepsilon}, \frac{\varepsilon_{22}}{Y_\varepsilon}, \left|\frac{\varepsilon_{12}}{S_\varepsilon}\right|\right) \tag{1}$$

with

$$X_\varepsilon = \begin{cases} \varepsilon_{LU}^{+} & \text{for} \quad \varepsilon_{11} > 0 \\ \varepsilon_{LU}^{-} & \text{for} \quad \varepsilon_{11} \le 0 \end{cases} ; \; Y_\varepsilon = \begin{cases} \varepsilon_{TU}^{+} & \text{for} \quad \varepsilon_{22} > 0 \\ \varepsilon_{TU}^{-} & \text{for} \quad \varepsilon_{22} \le 0 \end{cases} ; \; S_\varepsilon = \varepsilon_{LTU} \tag{2}$$

The ultimate failure stain in tension $()^{+}$ and in compression $()^{-}$ used in order to plot the contour plot for MSTRN is listed in the table in Fig. 4c.

3. Model

The STL surface representation of the inner surface obtained from a 3D optical scan of the brace is imported as a orphan shell into the commercial finite element mode Abaqus (Simulia, 2010) using the “STL Import” feature . Some part of the shell edge was included in the STL representation from the optical scan resulting in an L-shaped edge of the shell and was subsequently removed manually so they did not contribute artificial extra shell stiffness in the finite element model. In the two curved rods, see Fig 2a, where the fiber-reinforcement is placed to following the axial direction of the rods, a discrete material orientation was chosen, shown as the non dark blue part of Fig 2b. This was done by first choosing the surface of the rods and in here individual chose a selection of element edges following the axial direction of the rods. The composite layup was thereafter defined in this discrete material coordinate system. The top frontal part (the upper dark

blue part in Fig 2c) and the sole region (the lower dark blue part in Fig 2c) was kinematic coupled to two reference points which was used in order to prescribed the boundary conditions. All the degree of freedoms of the reference point in the sole region was fixed, while the reference point kinematic coupled to the upper part was prescribed with a forward horizontal deflection given by the x-direction in the coordinate system shown in Fig 2a. This was taken to simulate a step during normal gait. The coordinate system in Fig 2a was defined with the x-axis in the forward axial direction of the sole and the z-axis normal to the sole.

4. Results

Figure 5 show the horisontal load versus deflection curve representing a normal gait. The brace studied in the following full scale test is the “45-Carbon” which is a brace with twisted carbon glass webbing in the rods. The response of this brace is in Fig. 5 compared with three others material selections. Of this, the UD-carbon (folded untwisted carbon glass web) do give a slightly stiffer response while a UD-glass fibers reinforcment give a slightly softer response. The brace with no extra fiber rienforcement result en a significant softer but for the application still sufficiently stiff response. During the deformation, the center of the rods will move outward and rotate as it with a good eye and be seen at the two deformed shapes in Fig. 2b and 2c for $U = 58mm$ and $U = 76mm$, respectively.

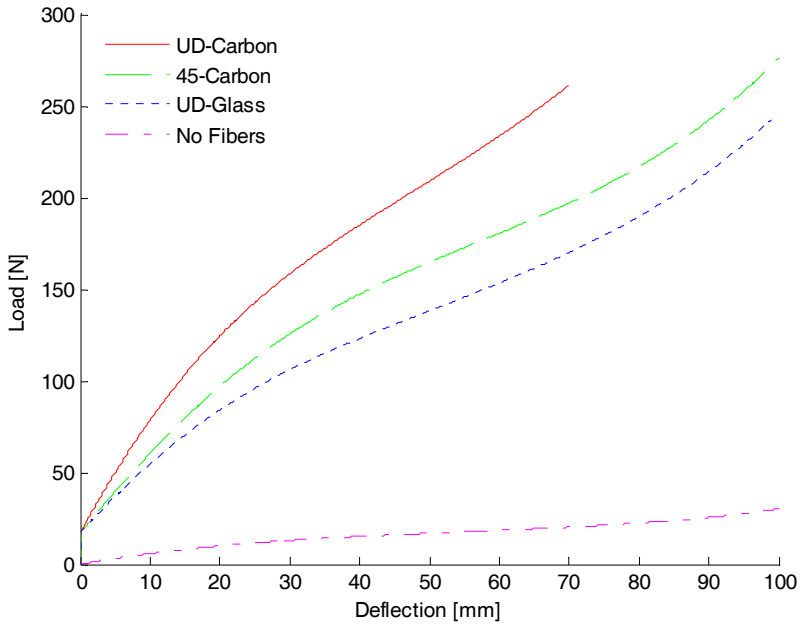

Figure 5. Load versus deflection curve for the four cases

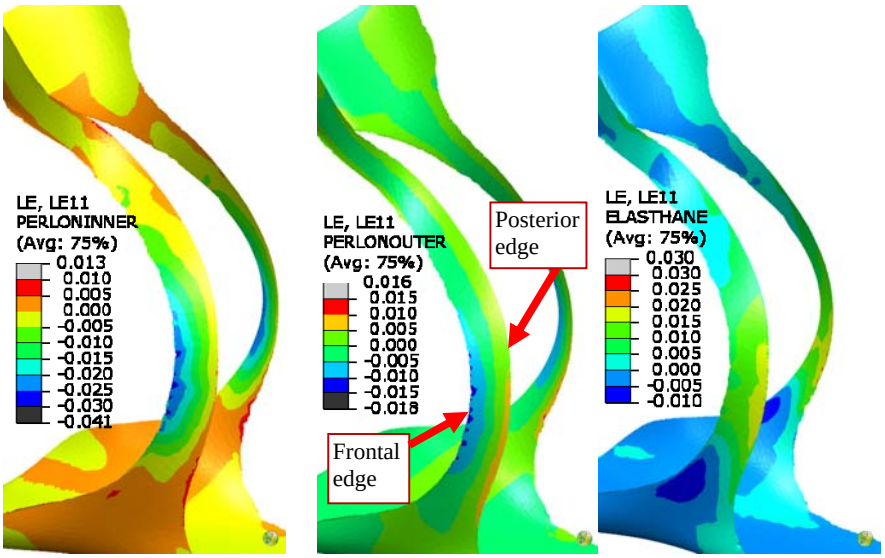

Figure 6. The axial strain in the rods for a brace with no fiber reinforcement at a deflection on $U = 58mm$ for a) the inner surface, b) the middle surface and c) the outer surface, respectively.

Figures 6a-c show the influence of the outward bending on the axial strain in the rods of the brace. The deformed brace with no extra fiber reinforcements at a horizontal deflection of the upperpart of the brace on $U = 58mm$ is shown where the strain is plotted in the local material coordinate system which a defined to follow the axial direction of the rods. Comparing the strain fields at the inner and the outer surfaces of the rods (Fig. 6a and Fig 6c) a transition for a overall negative to a overall possitive strain field corresponding to a outward bending of the deformed rod can be identified. Fig. 6b show on the other hand the axial strain field in the middle surface of the rods. This strain field is seen to go from a negative value at the frontal edge to a possitive value on the posterior edge corresponding the a forward bending of the rods. The the specific deformation stage, all the axial strains is found to be below 2-3% which compared with Fig. 3 is seen to be in the limite of allowed strains of the perlon and elasthane material.

Figures 7a-c show the contours of the "MSTRN" values, see equation (2), for the three cases with extra fiber reinforcements. The contours are shown for $U = 30mm$. For this deformation stage, the cases with an aligned carbon glass web (UD-Carbon) is found to be loaded a factor of more than 200% of the fiber strength while the loading of the twisted carbon glass web (45-Carbon) is around 160%. On the other hand, the unidirectional glass fiber reinforcement is found to just be loaded to the allowed level. The difference between the carbon and glass cases is mainly do to the fact that a glass fiber composite have a larger strain to failure value compared with a carbon fiber composite. Therefore, for a case where it is more a prescribed deformation level than a load level which give the design limites, the strong but more brittle carbon fibers may not be the most optimal material chose. It should be noted that the failure strain is sat to a realistic value resulting in fatigue failure of the fibers (Bech, 2011).

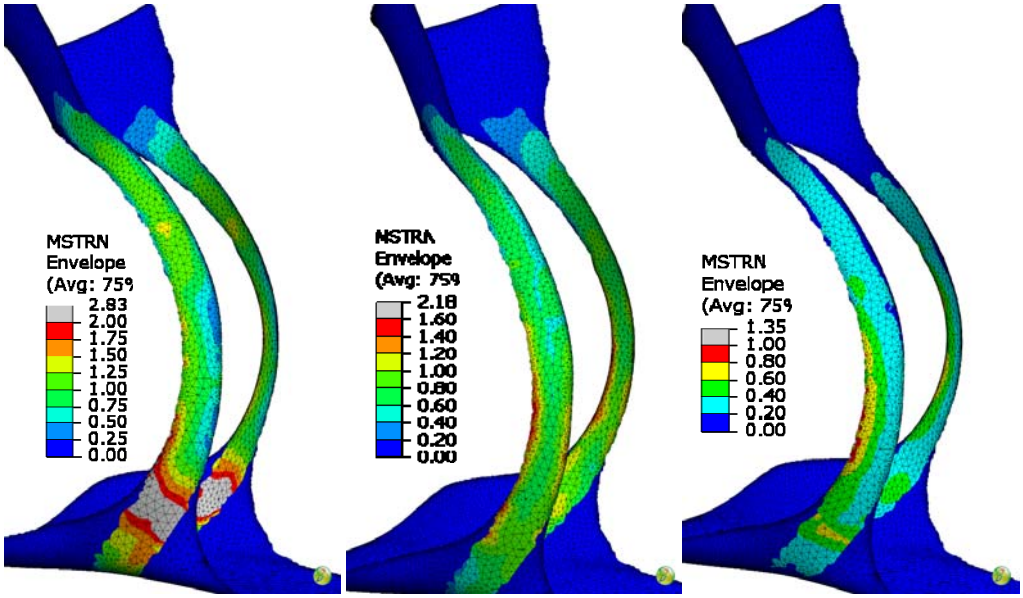

Figure 7. The through thickness maximum MSTRN at a deformation $U = 30mm$ for a) UD-Carbon, b) 45-Carbon and c) UD-Glass, respectively

5. Full scale test

The brace reinforced with the twisted carbon glass web has been tested in a full scale test. Before the test, rosette gauge has been mounted at four specific places on the surface of the lateral rod in the brace. Three strain gauges on the frontal surface and one on the back surface of the rod, see Fig. 8. At two different deformation stages, $U = 58mm$ and $U = 76mm$, the three in-plane strain components is extracted from the strain gauge measurements. The rosette gauges is oriented such that the 0° - normal strain is following the edge, and thereby for the case of FT, FM and BM the axial direction of the rod. In here, only the axial normal strain in the rods will be compared with the finite element simulation

Fig. 9 show a comparison of the measured normal strains, ε_{SG}, in the axial direction of the lateral rod with the corresponding strain extracted from the Abaqus simulations for the case with the twisted carbon glass fibre web. In the FM and BM point the effect of the outward bending of the rod can be seen both on the measurements and the simulations on the positive values of the strains on the outer surface and the negative value on the inner surface. Nevertheless, above in the point FT, a small negative strain is measured while a positive strain is predicted. Making the comparison, it may be kept in mind that the strain variation in the brace may be significantly influence on small variation in the geometry and in the loading direction. Nevertheless, strain of the same order of magnitude is achieved, comparing the finite element simulations with the full scale test.

Figure 8. Full scale test: a) zero position, b) Horizontal deflected $U = 58mm$, c) Horizontal deflected $U = 76mm$

.

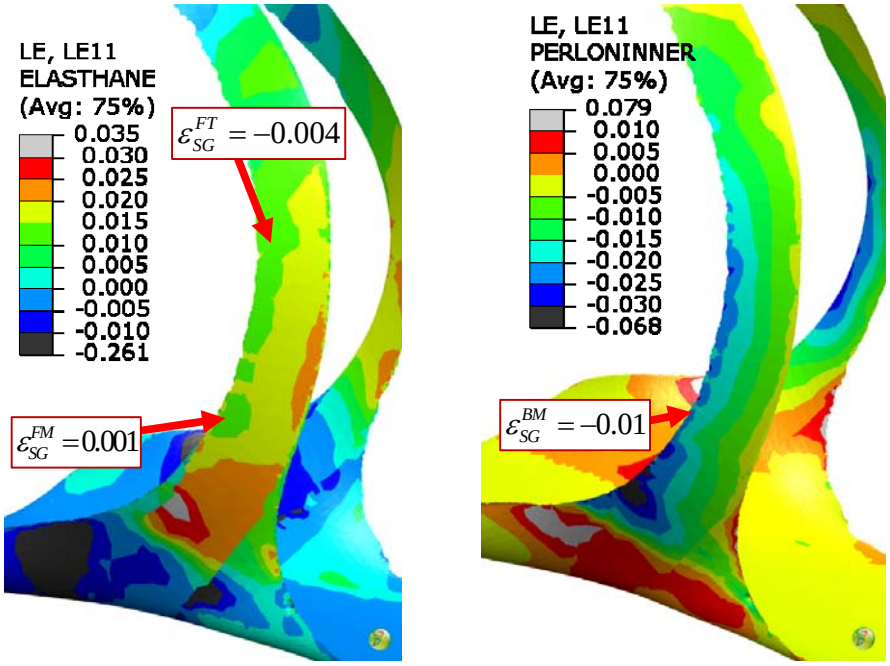

Figure 9. Predicted axial strains in the rod at the a) outer and b) inner surface for Carbon45 at a deflection on $U = 58mm$

6. Conclusion

The objective of this study was to investigate the deformation level of a person specific drop foot brace. The investigation show a rather complex deformation stage of the brace. Nevertheless, is has been demonstrated how the model can be used in order to optimize the material selection used for the brace in addition to give a overview of other effects influencing the straining of the material in the brace.

7. Reference

Bech, J.I., S. Goutianos, T.L. Andersen, R.K. Torekov and P. Brøndsted. 2011, "A New Static and Fatigue Compression Test Method for Composites". Strain,vol. 47, No. 1, 21-8.

Bojsen-Møller, F., "Bevægeapparatets anatomi", Foden, Munksgaard, København, 2005.

Flexbrace, 2010, Ortopæd Ingeniørene, Roskilde, Denmark, http://www.flexbrace.dk.

Kottnik, A.I., H.J. Hermens, A.V. Nene, et al., "A Randomized Controlled Trial af an Inplantable 2-Channel Peroneal Nerve Stimulator on Walking Speed and Activity in Poststroke Hemiplegia," Archives of Physical and Medicine Rehabilitation, vol. 88, pp. 971-978, 2007.

Murray, C. & Lopez, A. 2002, *The World Health Report 2002 - Reducing Risks, Promoting Healthy Life*, World Health Organization, http://www.who.int/whr/2002/en/2hr02_en.pdf.

Rubin, D.I., Kimmel, D.W. & Cascino, T.L. 1998, *Outcome of peroneal neuropathies in patients with systemic malignant disease*.Cancer, vol. 83, 1602-1606.

Simulia 2010, *Abaqus*/standard version 6.10 .

Wade, D.T., Wood, V.A., Heller, A., Maggs, J. & Hewer, R.L. 1987, *Walking after stroke measurement and recovery over the first 3 month*s. Scandinavian Journal of Rehabilitation and Medicine, vol. 19, 25-30.

Zebicon, 2002, Industrial 3D measuring and digitization, Billund, Denmark, http://www.zebicon.com.

Acknowledgements: The work has been financial supported by the Bio/Bio Composites projects under "Regional Growth Forum Zeeland". In addition, Lars Falkenman from Ortopæd Ingeniørerne, Roskilde, Denmark, is acknowledged for introducing the subject and for supply of materials and brace.